THE JOURNAL OF BIOLOGICAL CHEMISTRY
Vol. 272, No. 41, Issue of October 10, pp. 25468–25473, 1997

Printed in U.S.A.

Expression and Circular Dichroism Studies of the Extracellular Domain of the α Subunit of the Nicotinic Acetylcholine Receptor*

(Received for publication, April 21, 1997, and in revised form, July 23, 1997)

Anthony P. West, Jr.‡, Pamela J. Bjorkman§¶, Dennis A. Dougherty‡, and Henry A. Lester§‖

From the Divisions of ‡Chemistry and Chemical Engineering and §Biology and the ¶Howard Hughes Medical Institute, California Institute of Technology, Pasadena, California 91125

To provide material suitable for structural studies of the nicotinic acetylcholine receptor, we have expressed and purified the NH_2-terminal extracellular domain of the mouse muscle α subunit. Several constructs were initially investigated using *Xenopus* oocytes as a convenient small scale expression system. A fusion protein (α210GPI) consisting of the 210 NH_2-terminal amino acids of the α subunit and a glycosylphosphatidylinositol anchorage sequence conferred surface α-bungarotoxin binding in oocytes. Coexpression of α210GPI with an analogous construct made from the δ subunit showed no evidence of heterodimer formation. The α210GPI protein was chosen for large scale expression in transfected Chinese hamster ovary cells. The α210GPI protein was cleaved from these cells and purified on an immunoaffinity column. Gel and column chromatography show that the purified protein is processed as expected and exists as a monomer. The purified protein also retains the two distinct, conformation-specific binding sites expected for the correctly folded α subunit. Circular dichroism studies of α210GPI suggest that this region of the receptor includes considerable β-sheet secondary structure, with a small proportion of α-helix.

The nicotinic acetylcholine receptor (AChR)[1] is the best studied member of a large class of structurally related neurotransmitter-gated ion channels (1). This class includes both cation channels (acetylcholine and serotonin type 3 receptors) and anion channels (glycine, γ-aminobutyric acid type A, and an invertebrate glutamate receptor). Available data for some of these receptors suggest that each is a pentamer of homologous or identical subunits. Each subunit contains an NH_2-terminal extracellular domain (~200 residues) followed by four putative membrane-spanning domains. The regions between the second and third transmembrane domains (~15 residues) and after the fourth transmembrane domain (~9 residues) are also thought to be extracellular but do not appear to be critical for the folding of the large NH_2-terminal domain (see below). The high degree of sequence similarity among these subunits, especially in their extracellular domains, suggests that if the structure of any one was known, molecular modeling could be used to approximate the structures of the others.

Although there has recently been progress in obtaining structures of membrane proteins (particularly of bacterial membrane proteins) (2), many years of effort with *Torpedo* AChR have failed to yield crystals that diffract to high resolution. The highest resolution structural information on these receptors thus far is that obtained by Unwin (3, 4). Two-dimensional close-packed arrays of AChR in tubular membranes were prepared from the electric organ of *Torpedo marmorata*, a particularly rich source of muscle-type AChR, and examined using electron microscopy. From these studies a three-dimensional structure to 9 Å resolution (3) and a projection structure to 7.5 Å (4) were obtained. Although these data provide evidence for the presence of certain elements of secondary structure, obtaining atomic resolution structural information remains an important goal.

One approach that has been used successfully to obtain atomic resolution structures of membrane-bound receptors is to express these proteins heterologously in truncated, soluble forms. Because these fragments no longer contain long stretches of hydrophobic amino acids requiring detergent for solubilization, they crystallize more readily. The structures of the ligand binding domains of the human growth hormone receptor (5), the neonatal Fc receptor (6), and the T-cell receptor (7, 8) among others, have been determined in this way.

Although only about half the mass of AChR is extracellular, several recent studies suggest that the NH_2-terminal domain of a single subunit might be suited to this approach because the α subunit and various truncated forms of this subunit can fold independently of the other subunits. The assembly of the mouse muscle AChR has been studied extensively (9, 10). Each subunit is synthesized as a preprotein with an NH_2-terminal signal peptide directing translocation into the endoplasmic reticulum. Here the signal peptides are cleaved, and the subunits fold, become glycosylated, and are assembled into the final pentameric receptor. The α subunit acquires two conformation-dependent binding sites during the folding process but before assembly with the other subunits (11). One of these sites is the main immunogenic region, which is the epitope recognized by most experimentally derived antibodies and by a large fraction of the anti-AChR antibodies from patients with myasthenia gravis (12). The other binding site, which overlaps with the ligand binding site, is for the snake venom protein α-bungarotoxin (α-Btx). These binding sites are acquired simultaneously about 20 min after the α subunit is translated. After folding (or at least partial folding), subunit assembly occurs. Folded α subunits associate with either δ or γ subunits to form heterodimers. In studies of cells transfected with various combinations of subunits, it has been found that the αδ and αγ heterodimers have high affinity cholinergic ligand binding sites

* This work was supported by National Institutes of Health Grants NS-11756 and NS-34407, the California Tobacco-related Disease Research Program, and the Howard Hughes Medical Institute. The costs of publication of this article were defrayed in part by the payment of page charges. This article must therefore be hereby marked "*advertisement*" in accordance with 18 U.S.C. Section 1734 solely to indicate this fact.

‖ To whom correspondence should be addressed: Division of Biology, 156-29, California Institute of Technology, Pasadena, CA 91125. Tel.: 818-395-6872; Fax: 818-564-8709; E-mail: Lester@Caltech.edu.

[1] The abbreviations used are: AChR, acetylcholine receptor; α-Btx, α-bungarotoxin; CHO, Chinese hamster ovary; GPI, glycosylphosphatidylinositol.

and that the distinct agonist/antagonist profiles of these two heterodimers match those of the whole receptor (13).

Several studies have examined the effects of coexpression of truncated subunits with full-length subunits. Generally, subunits truncated after the first transmembrane domain (M1) have a dominant negative effect on the appearance of receptor on the plasma membrane, measured either electrophysiologically or by α-Btx binding (14, 15). The origin of this effect is the formation of a specific complex between full-length subunits and the truncated forms. These complexes neither form complete receptors nor undergo transport to the plasma membrane. These results indicate that the NH_2-terminal domains of AChR subunits contain regions that specifically recognize other subunits. Together with the observation that the α subunit is able to fold independently of the other subunits, these data suggest that the α subunit NH_2-terminal domain may be a viable target for structural investigation.

In the present experiments, we sought to produce the extracellular domains of AChR subunits in their native states in quantities sufficient for biochemical and structural studies. First with *Xenopus* oocytes and then with Chinese hamster ovary (CHO) cells, we expressed the truncated NH_2-terminal fragment of the α subunit fused with a sequence directing membrane anchorage via a glycosylphosphatidylinositol (GPI) linkage (16). By cleaving this protein from the membrane, we were able to obtain this portion of the AChR as a soluble protein. Toxin and antibody binding studies indicate that this fragment adopts a fold comparable to the corresponding region of the intact receptor. Circular dichroism (CD) studies reveal that this fragment of the receptor contains a large proportion of β-sheet secondary structure.

EXPERIMENTAL PROCEDURES

Reagents—Methionine sulfoximine was from Sigma, and peptide: *N*-glycosidase F was obtained from New England Biolabs. Phosphatidylinositol-specific phospholipase C from *Bacillus cereus* was expressed in *Escherichia coli* and purified by isolating periplasmic proteins by osmotic shock followed by ion exchange chromatography (17). Monoclonal antibody (mAb) 35 was purified from the supernatant of cultures of hybridoma cells (American Type Culture Collection, TIB 175) by ammonium sulfate precipitation. An immunoaffinity column was prepared by coupling mAb 35 to CNBr-activated Sepharose (Pharmacia Biotech Inc.) according to the manufacturer's instructions. mAb 210 was the gift of Jon Lindstrom (University of Pennsylvania). All other chemicals were reagent grade.

Construction of GPI-linked Forms—Molecular cloning experiments were performed by standard methods (18). Full-length cDNAs coding for the α and δ subunits of the mouse muscle AChR in pAMV-PA have been described (19). The chick α7 subunit was obtained from M. Ballivet (University of Geneva) and transferred to plasmid pAMV-PA. Site-directed mutagenesis was used to create unique restriction sites preceding transmembrane domain 1, and an insert containing the GPI anchor signal from human placental alkaline phosphatase (20) was ligated to give a vector encoding the fusion protein. The three constructs we made were α210GPI, δ226GPI, and α7-208GPI (where the numbers refer to the last amino acid included in the truncated subunit as numbered from the first amino acid of the mature protein). These vectors were linearized with *Not*I, and mRNA was transcribed using the T7 polymerase mMessage mMachine kit from Ambion (Austin, TX). For mammalian expression, the coding region for α210GPI was subcloned into the vector pBJ5.GS (21). This vector contains a strong simian virus 40/human T-lymphotropic virus type1 hybrid promoter for constitutive expression and the glutamine synthetase minigene (obtained from Celltech, Berkshire, U. K.), which can be used as a selectable marker and means of gene amplification (22). This marker allows transfected cells to grow in glutamine-free medium in the presence of methionine sulfoximine, an inhibitor of the cell's native glutamine synthetase.

Oocyte Preparation and Injection—Oocytes were removed from *Xenopus laevis* as described previously (23) and maintained at 18 °C in a standard solution (ND-96) consisting of 96 mM NaCl, 2 mM KCl, 1 mM $MgCl_2$, 1.8 mM $CaCl_2$, and 5 mM Hepes supplemented with 2.5 mM sodium pyruvate, 50 mg/ml gentamicin, and 0.6 mM theophylline, pH 7.5. Oocytes were microinjected (50 nl) with mRNA in three groups: α210GPI (25 ng of mRNA), α210GPI (12.5 ng) plus δ226GPI (25 ng), and α7-208GPI (25 ng).

Surface expression of α-Btx binding sites was determined by incubating intact oocytes (60 h postinjection) for 2 h at room temperature with 0.66 nM ^{125}I-α-Btx (2000 Ci/mmol; Amersham Corp.) in ND-96 with 1 mg/ml bovine serum albumin. To assay for antagonist-displaceable α-Btx binding, oocytes were incubated with α-Btx in the presence of 200 μM *d*-tubocurarine chloride. Because α-Btx binds nearly irreversibly, this experiment measures the reduction in initial rate of α-Btx binding.

Cell Culture and Transfection—CHO K1 cells were grown in α minimum essential medium (Irvine Scientific) supplemented with 5% fetal bovine serum, 2 mM glutamine, and 100 units/ml penicillin/streptomycin. Stably transfected cell lines were made as described previously (24). In brief, the pBJ5.GS.α210GPI expression vector was transfected into CHO cells by a liposome (LipofectAmine)-mediated method (Life Technologies, Inc.). Two days after transfection the cells were placed in α minimum essential medium with 5% dialyzed fetal bovine serum without glutamine and with 25 μM methionine sulfoximine. Individual clones were isolated, and the expression level was determined by ^{125}I-α-Btx binding and by flow cytometry. Attempts to improve expression levels by amplification of the glutamine synthetase gene with higher methionine sulfoximine concentrations were unsuccessful. The highest expressing cell line was grown in 10-cm plates and in a Cell Pharm hollow-fiber bioreactor device (Unisyn Fibertec, San Diego).

Flow Cytometric Analysis—Cells released from plates using versene were incubated with a solution of mAb 210, washed, and then treated with a fluorescein-conjugated goat $F(ab)'_2$ anti-rat IgG (Life Technologies, Inc.). Flow cytometric analyses were carried out on a Coulter Epics Elite flow cytometer/cell sorter.

Purification of α210GPI—To release α210GPI from the cell surface, purified phosphatidylinositol-specific phospholipase C (50 μg) was injected in the cell compartment of the bioreactor or added to dishes containing the transfected CHO cells. After 2 h, the cell medium (250 ml) was collected and filtered. This solution was passed over the mAb 35 affinity column at a flow rate of 50 ml/h at 4 °C, and the column was washed with 50 ml of phosphate-buffered saline. Elution of α210GPI from the column was accomplished with 10 ml of a low pH solution (50 mM sodium citrate, pH 3.0, 1 M NaCl). The eluant was collected into 1 M Tris, pH 8.0 (3 ml), and concentrated to approximately 0.2 mg/ml by ultrafiltration using an Amicon Centriplus-10 (M_r cutoff of 10,000). The concentrated protein solution (0.2–0.5 ml) was applied to a fast protein liquid chromatography Superdex 75 column equilibrated with Tris-buffered saline or with 5 mM sodium phosphate buffer. This column was run at room temperature with a flow rate of 0.1 ml/min. The fraction containing the α210GPI protein was again concentrated with an Amicon Centriplus-10.

The α-Btx binding activity of purified, soluble α210GPI was measured by immobilization of this protein on mAb 35-agarose beads followed by binding of ^{125}I-α-Btx. A solution containing 10–100 ng of α210GPI was added to a suspension of 15 μl of mAb 35-agarose beads in a 1.5-ml microcentrifuge tube. After 30 min of incubation, the suspension was centrifuged at 2,500 rpm. The supernatant was removed and replaced with a solution of unlabeled α-Btx and ^{125}I-α-Btx of known specific activity in phosphate-buffered saline with 1 mg/ml bovine serum albumin. After a 2-h incubation, the beads were again centrifuged and then washed three times with 1 ml of phosphate-buffered saline by repeated resuspension and centrifugation. The bound ^{125}I-α-Btx was measured using a γ counter. All incubations were at room temperature with agitation.

NH_2-terminal Amino Acid Sequencing—Protein eluted from the mAb 35 affinity column was electrophoresed on a 10% SDS-polyacrylamide gel and electroblotted in a Bio-Rad Trans-Blot system onto a polyvinylidene difluoride membrane. The major band visible by Coomassie staining was cut out and analyzed by an Applied Biosystems model 476A sequencer.

Circular Dichroism—Spectra were collected using an AVIV CD spectrometer model 62A DS. Protein concentration was determined by UV absorbance at 280 nm, taking into account the amino acid content of α210GPI and light scattering (25). Cuvettes with path lengths of 0.1 or 1.0 cm were used, and the mean residue ellipticity (degrees·cm^2/dmol) was determined using a mean residue weight of 116. Spectra were recorded at 20 °C from 250 to 185 nm and were determined as the average of five scans. Two methods were used to estimate secondary structure content: (i) the relationship between the mean residue ellipticity at 208 nm and the α-helical content given by Greenfield and Fasman (26) and (ii) the CONTIN program (27), which fits the spectrum

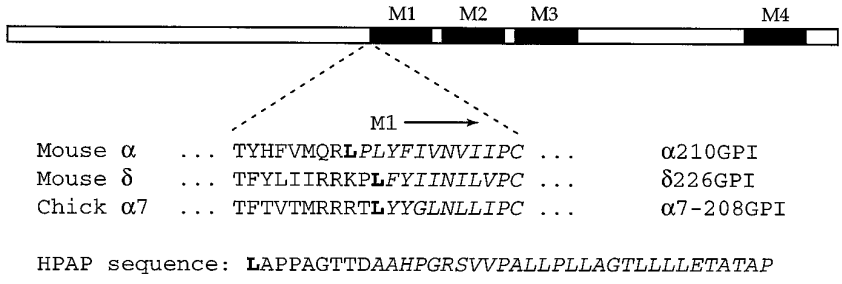

FIG. 1. **Constructs used in these experiments.** *Bold* residue indicates point of truncation and fusion to the human placental alkaline phosphatase (*HPAP*) sequence. Residues in *italics* have been removed by truncation or, in the case of the human placental alkaline phosphatase sequence, are removed from the expressed protein when the GPI anchor is attached.

between 240 nm and 190 nm, using the protein standards suggested by Sreerama and Woody (28).

RESULTS

Expression in Oocytes—We made three constructs containing truncated subunit fragments fused to the human placental alkaline phosphatase GPI anchorage sequence: α210GPI, δ226GPI, and α7-208GPI. Fig. 1 shows the sequences of the constructs we tested. In addition to the fusion proteins made from the extensively studied muscle AChR, we chose to make a fusion protein with the neuronal α7 subunit because it forms functional homomeric receptors when expressed heterologously (29). Thus, one or more α7 subunits are able to form ligand binding sites without the presence of other types of subunits.

These constructs were studied by microinjection of mRNA into *Xenopus* oocytes followed by α-Btx binding. Preliminary experiments indicated that expression of either α210GPI or α7-208GPI led to the appearance of α-Btx binding sites on the oocyte surfaces. As expected for proteins attached to the plasma membrane by GPI anchors, these α-Btx binding sites could be cleaved selectively from the cell surface by treatment with phosphatidylinositol-specific phospholipase C (data not shown). We next examined whether coexpression of α210GPI and δ226GPI, or the expression of α7-208GPI alone, would lead to the formation of a high affinity ligand binding site, detectable as antagonist-inhibitable α-Btx binding. The results of the α-Btx binding experiment are shown in Fig. 2. Neither expression of α210GPI alone, nor coexpression of α210GPI and δ226GPI, led to development of a ligand binding site, as evidenced by the failure of the nicotinic antagonist *d*-tubocurarine to prevent α-Btx binding. In contrast, α7 expressed alone showed antagonist inhibition of α-Btx binding.

Expression in Mammalian Cells and Purification—Because the α210GPI protein expressed relatively well in oocytes and could be cleaved from the surface, we wished to obtain greater quantities of this protein for further characterization. To scale up the production of the α210GPI protein, we expressed this protein in stably transfected mammalian cells. Cell lines were made using the glutamine synthetase-based expression system (22). After selection and cloning of high expressing cell lines, we were able to produce the protein on a 10–100-μg scale. This modest expression level may reflect the limited surface area available for GPI-linked proteins or may be the result of the previously observed inefficient folding of the α subunit (11). Flow cytometric analysis (Fig. 3*A*) demonstrates that α210GPI is expressed on the surface of transfected cells and shows that the majority of cells have uniform (± 35%) levels of protein/cell.

The most common method of purifying AChR employs binding to a snake toxin affinity column followed by elution with a nicotinic agonist. Because the α210GPI protein lacks an agonist site and the toxin-α subunit binding is nearly irreversible, we sought an alternative purification strategy. We developed an immunoaffinity-based purification protocol similar to that used for isolation of a (non-α-Btx binding) chick neuronal AChR (30). After phosphatidylinositol-specific phospholipase C cleavage from cells grown in dishes or the bioreactor, the α210GPI

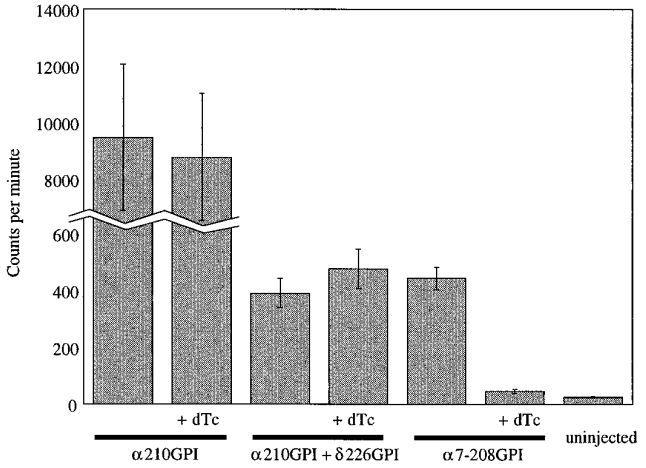

FIG. 2. **Surface α-Btx binding by oocytes injected with GPI-linked constructs.** Pools of oocytes were incubated with 0.66 nM ^{125}I-α-Btx either in the absence or presence (+*dTc*) of 200 μM *d*-tubocurarine.

protein was purified from the serum-containing medium on a mAb 35 immunoaffinity column. Low pH elution resulted in the separation of α210GPI from almost all contaminating serum proteins. Gel filtration chromatography was then performed to isolate (monomeric) α210GPI from larger molecular weight proteins (including aggregated α210GPI). This protocol allowed us to obtain the protein in a nearly pure state, suitable for various biochemical studies. The specific α-Btx binding of the purified material rebound to mAb 35-agarose beads was about 16 nmol/mg, which was about 40% of the value calculated on the basis of protein mass.

Like the native receptor α subunit, the α210GPI protein is glycosylated. Fig. 3*B* shows the change in apparent molecular mass on an SDS-polyacrylamide gel when the purified material is enzymatically deglycosylated by peptide:*N*-glycosidase F. A sample of the α210GPI protein was subjected to protein microsequencing (data not shown). The sequence obtained, SEHETRLVAKLF, exactly matches the NH_2-terminal 12 residues of the mature α subunit, verifying that the NH_2-terminal signal peptide had been processed correctly. When bound to mAb 35-agarose beads, the purified material binds α-Btx with a K_d estimated by Scatchard analysis of about 3 nM (data not shown), which falls within the range of values reported for the native receptor (12). The properties of the α210GPI protein were examined by gel filtration. As shown in Fig. 4, the protein behaves as a monomer. The apparent molecular mass of the complex of α210GPI with α-Btx (an 8-kDa protein) was approximately 10 kDa larger, as expected for a one-to-one complex. An additional gel filtration experiment with ^{125}I-α-Btx demonstrated that the radioactive label does elute at the ~45-kDa peak (data not shown).

Circular Dichroism Studies—We used CD to probe the secondary structure of the expressed extracellular domain. The CD spectrum of a given protein can be approximated as the

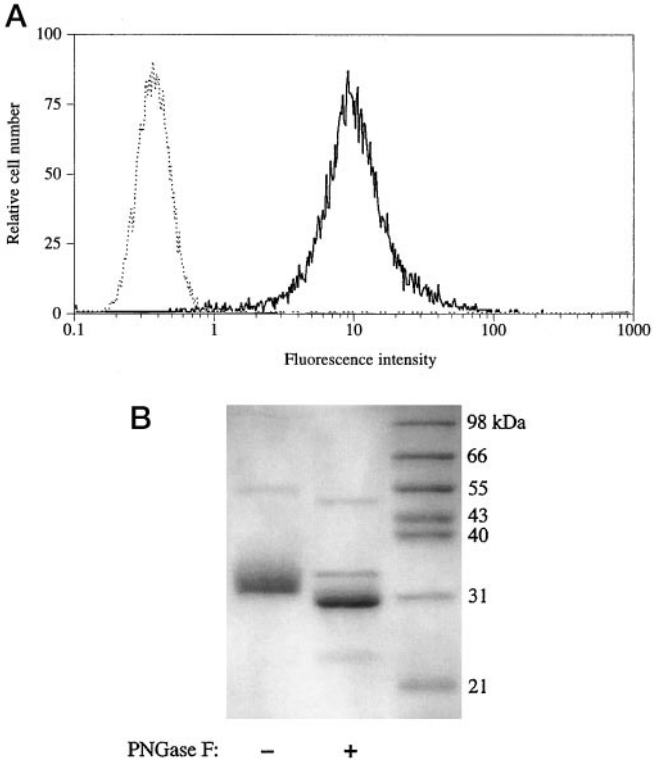

FIG. 3. **Expression of α210GPI in CHO cells.** *Panel A*, flow cytometric analysis of the α210GPI expressed on CHO cells. Staining of transfected cells by mAb 210; secondary antibody is fluorescein-labeled goat $F(ab')_2$ anti-rat IgG. *Solid trace*, transfected cell line expressing α210GPI; *dotted trace*, untransfected CHO cells. *Panel B*, Coomassie-stained 12% SDS-polyacrylamide gel electrophoresis of purified α210GPI, showing the effect of deglycosylation by peptide:*N*-glycosidase F. Peptide:*N*-glycosidase F appears as the new band ~34 kDa.

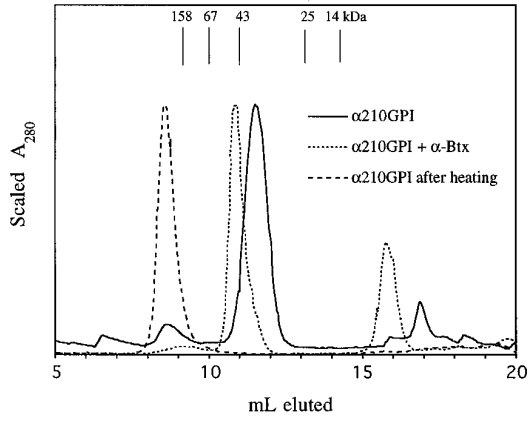

FIG. 4. **The extracellular domain of the AChR α subunit exists as a monomer competent to bind α-bungarotoxin, as demonstrated by gel filtration chromatography.** Gel filtration profiles (fast protein liquid chromatography Superdex 75 column in 5 mM sodium phosphate buffer, pH 7.5, flow rate 0.1 ml/min) of three samples: purified α210GPI, a mixture of α210GPI with α-Btx (1:2 mol ratio), and thermally denatured α210GPI. *Traces* have been scaled by factors of 1.0, 2.6, and 2.3, respectively, to yield equal peak amplitudes. Samples containing 10–20 μg of α210GPI/run were passed through a 0.2-μm filter immediately before injection onto the column.

sum of characteristic contributions from different elements of secondary structure (26). Fig. 5*A* shows the CD spectrum of α210GPI compared with the published CD spectrum of the complete AChR ($\alpha_2\beta\gamma\delta$; Fig. 5*B*) (31). The strong negative ellipticities seen around 208 nm and 220 nm for the whole AChR indicate considerable α-helical content. The CD spectrum of α210GPI does not show this strong α-helical signature but

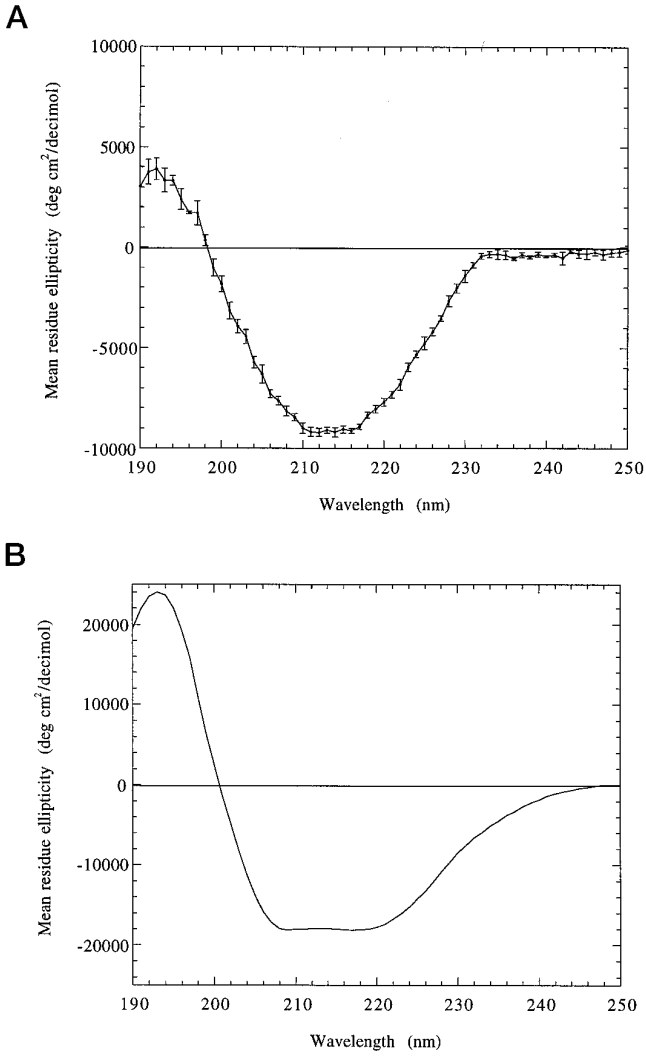

FIG. 5. *Panel A*, far UV CD spectrum of α210GPI. *Panel B*, far UV CD spectrum of whole AChR. Reprinted from Ref. 31 with permission.

instead shows the characteristics of a spectrum of a protein composed of largely β-sheet structure.

We compared the predicted secondary structure content of α210GPI with that of whole AChR using two methods of CD spectral analysis. The method of Greenfield and Fasman (26) estimates that α210GPI contains 14% α-helix compared with 48% for whole AChR. Analysis using the CONTIN program (27) suggests that α210GPI contains 12% α-helix, 51% β-sheet, 18% β-turn, and 20% irregular structure. For the spectrum of whole AChR, this method estimates 48% α-helix, 26% β-sheet, 13% β-turn, and 12% irregular structure. The estimates of the α-helical content of whole AChR exceed that calculated by Mielke and Wallace, who reported 22–29% α-helix, but others have noted that their estimate appears to be low based on the reported spectrum (32). In a review of the results of several spectroscopic methods, it has been suggested that complete AChR has close to 40% α-helix (33).

The thermal denaturation behavior of α210GPI was also investigated. When the protein was heated, a small but reproducible change in the CD spectrum was observed. Fig. 6 shows the spectra of α210GPI before, during, and after heating. Surprisingly, we do not observe a complete melting of the secondary structure of the protein. Because the spectra before and after melting differ, an irreversible change occurs. The most prominent change in the spectrum occurred in the region around 230 nm. Fig. 7 shows the change in ellipticity at 231 nm

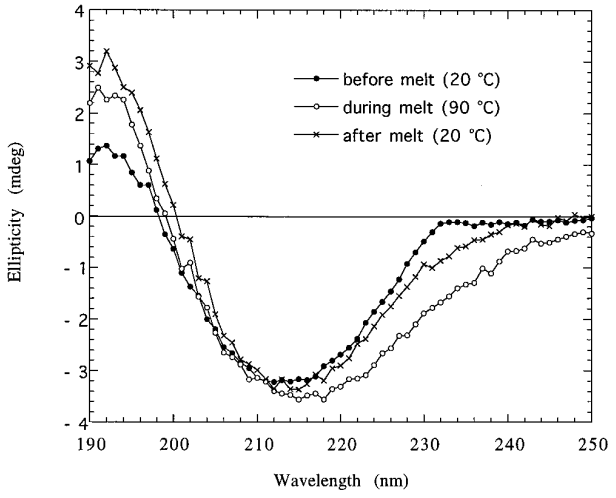

FIG. 6. **CD spectra of α210GPI before, during, and after heating.**

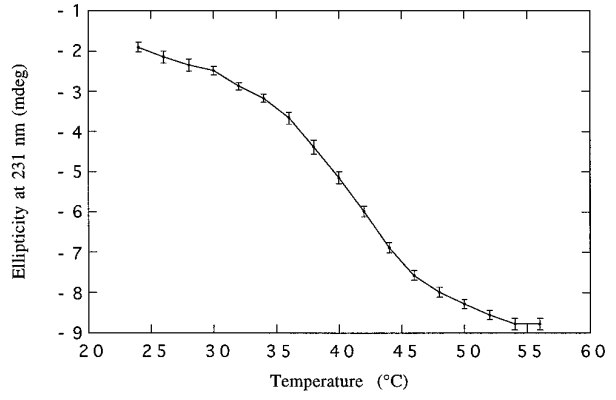

FIG. 7. **Temperature dependence of the ellipticity at 231 nm.** Data were obtained by increasing the temperature of the sample in 2 °C steps, equilibrating for 90 s, and measuring the ellipticity over a period of 90 s.

as the protein was heated from 24 to 56 °C. After thermal denaturation, the α210GPI protein no longer behaved as a monomer on gel filtration (Fig. 4). Separate experiments (not shown) indicate that the protein also becomes inactive in the α-Btx/mAb 35 assay when heated in this temperature range.

DISCUSSION

The α210GPI protein expresses well in oocytes and leads to the accumulation of surface α-Btx binding sites. Encouraged by this, we expressed and purified this protein on a larger scale using CHO cells. We are confident that the molecule we have purified, α210GPI, is folded correctly for the following reasons: (i) the material was affinity purified using a conformation-specific antibody; (ii) both the main immunogenic region epitope and the α-Btx binding site were present in the purified material; (iii) gel filtration results demonstrate that α210GPI behaves as a monomer and that it forms a complex with α-Btx with a slightly greater apparent molecular weight; and (iv) the α-Btx/mAb 35 binding activity of α210GPI is eliminated by thermal denaturation.

If about 15% of α210GPI is in an α-helical conformation, this represents approximately 33 amino acids. The sum of the lengths of these helices would be roughly 50 Å. In the 9 Å resolution electron microscopy structure, the extracellular portion of AChR contained three resolvable rods per subunit, approximately in the middle of that portion of the receptor (3). These rods in the electron density map appear to extend over at least 12 Å each. We thus consider our data to be compatible with the three α-helices identified in the extracellular domain of AChR. Our data also suggest that there is little or no α-helical structure elsewhere in the NH_2-terminal domain of AChR, implying that the remainder of the structure may be composed largely of β-sheet. This is in agreement with an early amphipathic analysis of AChR sequences which predicted the extracellular domain of AChR to contain extensive β-sheet structure (34).

When one considers the constraints that our data may place on the structure of AChR, an important issue is whether the secondary structures of the extracellular domains of the other subunits are largely the same as that for the α subunit. The high degree of sequence similarly (35–40% identity) and the results from electron microscopy studies suggest that such an assumption is reasonable, although there is little direct experimental evidence to address this question. With this caveat, our data suggest that the nonextracellular portion of AChR must have a relatively large proportion of α-helical structure if one is to reconcile these results with the previous CD spectrum of the entire receptor. Unfortunately, without knowledge of the secondary structure of the intracellular domain, no conclusions with respect to the structure of the transmembrane domains can be made.

The most prominent change in the CD spectrum which occurs upon heating is the appearance of negative ellipticity around 230 nm. The relatively flat spectrum from 230–240 nm, a region that should have negative ellipticity because of the β-sheet signal, suggests that there is an element of structure giving a positive ellipticity in this region. A positive component in this region is a feature of aromatic and/or disulfide chromophores, which can acquire rotational strength around 230 nm when they are in specific chiral environments in proteins (35). Notably, α210GPI is unusually rich in aromatic amino acids; it has 10 tyrosines and 8 tryptophans, about twice the expected number based on the average amino acid content of soluble proteins.

The apparent robustness of the α210GPI *secondary* structure to thermal denaturation is not unprecedented. For example, when bovine β-lactoglobulin A, a β-sheet-rich protein, is thermally denatured, the effect on the secondary structure (as measured by CD) is very small (36). It has been proposed that the aggregation/misfolding of many proteins is associated with the formation of intermolecular β-sheet structures (36, 37). The relatively low temperature required to cause loss of binding activity of α210GPI and the inefficient folding of the α subunit *in vivo* (with most of the newly synthesized α subunit appearing as non-α-Btx-binding aggregates) suggests that the α subunit is susceptible to this form of misfolding.

We contend that the lower than expected specific binding of α-Btx by the purified α210GPI is not likely to change substantially our estimates of the secondary structure. We consider the possible causes for the low specific binding. (i) If the α210GPI is contaminated with some denatured protein, then the recorded CD is a mixture of the folded and unfolded material. However, the spectrum of the heat-denatured protein is not markedly dissimilar from that of the correctly folded material. Therefore, admixture of some fraction of unfolded material will have little effect on the secondary structure estimates. (ii) If the protein concentration measurement is too high, this could increase the mean residue ellipticity substantially. Nevertheless, the shape of the spectrum, which is not very characteristic of α-helix, would be unchanged. The measurement of protein concentration by UV is reported to be accurate within about 10% (25). (iii) The measured specific binding may be slightly low because of occlusion of the α-Btx binding site by the antibody resin or by loss during washing steps.

The absence of a ligand binding site on oocytes expressing only α210GPI agrees with previous studies (11) showing that although the (complete) α subunit binds α-Btx with high affinity, it lacks the conventional ligand binding site of AChR. This site forms only when the muscle α subunit is coexpressed with either the δ or γ subunit (13). There is no obvious explanation for the failure of α210GPI and δ226GPI to form the ligand binding site when coexpressed. Coexpression of δ226GPI with α210GPI led to a much lower level of surface expression compared with α210GPI alone, even taking into account the reduced amount of α210GPI mRNA injected. Thus expression of δ226GPI may interfere with surface expression of α210GPI by an unknown mechanism. These findings are very similar to results reported by Hall and colleagues (38). In contrast, binding of α-Btx to α7-208GPI was inhibited by *d*-tubocurarine, indicating the formation of a ligand binding site and thus suggesting oligomerization of this protein (extrapolating from studies on the muscle receptor). Also, it has been reported (39) that oligomerization of α7 subunits is required for formation of the α-Btx binding site. It will thus be interesting to express and characterize α7-208GPI in future experiments.

Acknowledgments—We thank David Penny for help with the Cell Pharm expression, Shelley Diamond for assistance with flow cytometry, Steve Mayo for assistance with the CD experiments, and Jon Lindstrom for providing mAb 210.

REFERENCES

1. Karlin, A., and Akabas, M. H. (1995) *Neuron* **15,** 1231–1244
2. White, S. H. (ed) (1994) *Membrane Protein Structure: Experimental Approaches*, Oxford University Press, New York
3. Unwin, N. (1993) *J. Mol. Biol.* **229,** 1101–1124
4. Unwin, N. (1996) *J. Mol. Biol.* **257,** 586–596
5. Devos, A. M., Ultsch, M., and Kossiakoff, A. A. (1992) *Science* **255,** 306–312
6. Burmeister, W. P., Gastinel, N. E., Simister, N. E., Blum, M. L., and Bjorkman, P. J. (1994) *Nature* **372,** 336–343
7. Garcia, K. C., Degano, M., Stanfield, R. L., Brunmark, A., Jackson, M. R., Peterson, P. A., Teyton, L., and Wilson, I. A. (1996) *Science* **274,** 209–219
8. Garboczi, D. N., Ghosh, P., Utz, U., Fan, Q. R., Biddison, W. E., and Wiley, D. C. (1996) *Nature* **384,** 134–141
9. Green, W. N., and Millar, N. S. (1995) *Trends Neurosci.* **18,** 280–287
10. Blount, P., and Merlie, J. P. (1991) *Curr. Top. Membr.* **39,** 277–294
11. Blount, P., and Merlie, J. P. (1988) *J. Biol. Chem.* **263,** 1072–1080
12. Conti-Tronconi, B. M., McLane, K. E., Raftery, M. A., Grando, S. A., and Protti, M. P. (1994) *Crit. Rev. Biochem. Mol. Biol.* **29,** 69–123
13. Blount, P., and Merlie, J. P. (1989) *Neuron* **3,** 349–357
14. Verrall, S., and Hall, Z. W. (1992) *Cell* **68,** 23–31
15. Sumikawa, K., and Nishizaki, T. (1994) *Mol. Brain Res.* **25,** 257–264
16. Lin, A. Y., Devaux, B., Green, A., Sagerstrom, C., Elliott, J. F., and Davis, M. M. (1990) *Science* **249,** 677–679
17. Koke, J. A., Yang, M., Henner, D. J., Volwerk, J. J., and Griffith, O. H. (1991) *Protein Expression Purif.* **2,** 51–58
18. Sambrook, J., Fritsch, E. F., and Maniatis, T. (1989) *Molecular Cloning: A Laboratory Manual*, 2nd Ed., Cold Spring Harbor Laboratory, Cold Spring Harbor, NY
19. Nowak, M. W., Kearney, P. C., Sampson, J. R., Saks, M. E., Labarca, C. G., Silverman, S. K., Zhong, W., Thorson, J., Abelson, J. N., Davidson, N., Schultz, P. G., Dougherty, D. A., and Lester, H. A. (1995) *Science* **268,** 439–442
20. Kam, W., Clauser, E., Kim, Y. S., Kan, Y. W., and Rutter, W. J. (1985) *Proc. Natl. Acad. Sci. U. S. A.* **82,** 8715–8719
21. Gastinel, L. N., Simister, N. E., and Bjorkman, P. J. (1992) *Proc. Natl. Acad. Sci. U. S. A.* **89,** 638–642
22. Bebbington, C. R., and Hentschel, C. C. G. (1987) in *DNA Cloning: A Practical Approach* (Glover, D. M., ed) Vol. III, pp. 163–188, IRL Press, Oxford
23. Quick, M. W., and Lester, H. A. (1994) in *Ion Channels of Excitable Cells* (Narahashi, T., ed) pp. 261–279, Academic Press, San Diego
24. Wang, W.-C., Zinn, K., and Bjorkman, P. J. (1993) *J. Biol. Chem.* **268,** 1448–1455
25. Mach, H., Middaugh, C. R., and Lewis, R. V. (1992) *Anal. Biochem.* **200,** 74–80
26. Greenfield, N., and Fasman, G. D. (1969) *Biochemistry* **8,** 4108–4116
27. Provencher, S. W., and Glockner, G. (1981) *Biochemistry* **20,** 33–37
28. Sreerama, N., and Woody, R. W. (1993) *Anal. Biochem.* **209,** 32–44
29. Couturier, S., Bertrand, D., Matter, J. M., Hernandez, M. C., Bertrand, S., Millar, N., Valera, S., Barkas, T., and Ballivet, M. (1990) *Neuron* **5,** 847–856
30. Whiting, P. J., and Lindstrom, J. M. (1986) *Biochemistry* **25,** 2082–2093
31. Mielke, D. L., and Wallace, B. A. (1988) *J. Biol. Chem.* **263,** 3177–3182
32. Wu, C. C., Sun, X. H., and Yang, J. T. (1990) *J. Protein Chem.* **9,** 119–126
33. Methot, N., McCarthy, M. P., and Baenziger, J. E. (1994) *Biochemistry* **33,** 7709–7717
34. Finer-Moore, J., and Stroud, R. (1984) *Proc. Natl. Acad. Sci. U. S. A.* **81,** 155–159
35. Perczel, A., Park, K., and Fasman, G. D. (1992) *Proteins Struct. Funct. Genet.* **13,** 57–69
36. Griffin, W. G., Griffin, M. C. A., Martin, S. R., and Price, J. (1993) *J. Chem. Soc. Faraday Trans.* **89,** 3395–3406
37. Speed, M. A., Wang, D. I. C., and King, J. (1996) *Nature Biotech.* **14,** 1283–1287
38. Wang, Z. Z., Hardy, S. F., and Hall, Z. W. (1996) *J. Cell Biol.* **135,** 809–817
39. Anand, R., Peng, X., and Lindstrom, J. (1993) *FEBS Lett.* **327,** 241–246